

Reliability Based Critical infrastructure upgrade with photovoltaic integration and Strategic energy storage.

Mark Abuongor Ibuya

Department of Electrical and Electronics Engineering, University of Birmingham, B15 2TT, Birmingham, United Kingdom

DOI: 10.29322/IJSRP.12.02.2022.p12259
<http://dx.doi.org/10.29322/IJSRP.12.02.2022.p12259>

Paper Received Date: 29th January 2022
Paper Acceptance Date: 08th February 2022
Paper Publication Date: 19th February 2022

Abstract: Increased penetration of renewables to the transmission network with energy storage systems has increased the need for extended reliability assessment of load points of transformers and transmission lines. Solar power intermittency limits its significance in maximum integration and dependence by utilities. Therefore, its necessary to determine PV and energy storage levels to improve essential infrastructure reliability. The essential component's reliability is greatly influenced by the location PV and BESS. In this paper, the Markov modelling technique is adopted in designing both photovoltaic systems and BESS stochastic models. The model is used for reliability improvements studies of critical points. The paper is focused with PV and BESS locations and penetration levels influence on reliability improvements. This is achieved by using the failure and repair rates of photovoltaic and battery storage adopted in determining state probabilities and frequencies. The IEEE 24 bus system is used to evaluate load point reliability for different test case scenarios of photovoltaic integration and energy storage in Digsilent reliability tool Software. The simulation results indicate that integration of PV and BESS improves system reliability and load point reliability of critical infrastructures.

However, integration of PV and BESS at different locations results in reduced reliability due to network overloading and solar intermittency effects. The network maximum PV and BESS penetration level is determined to be 32.5%, above which system failure occurs.

Keywords

BESS, Composite system reliability, Digsilent, Energy storage, Photovoltaic Markov modelling, Load point Indices, System Indices

1. Introduction

United Nations report predicts that 66% of the world's population will be in urban areas by 2050[1]. This report implies that the energy demand will continuously increase, especially composite system generation, to meet rising industry demands. For example, the UK energy demand market was supplied halfway by renewables in 2017 for the first time in history.

The total grid power system capacity has increased from 300MW in 2000 to about 67 GW in 2011 exponentially[2] and has been growing ten-fold to date. Therefore, composite reliability analysis of power systems with photovoltaic integration and energy storage is vital for better utilization and security in the electrical power supply. This analysis involves determining penetration levels while assessing critical infrastructure and system reliability for continuous power supply.

Reliability is the probability that a given system or

component performs as expected during a specific period. Reliability analysis classifies components as either repairable or non-repairable.

Repairable system availability is the given specific time within which it's under operation before failing and repair again. For non-repairable systems, availability is represented by the valuable time before failure sets in[3]. The power system reliability is influenced by power availability, load variations, switch/protective gear, equipment failure/repair rates, currents limits, and alternative feeders availability[3]. Reliability categories are illustrated in figure 1.

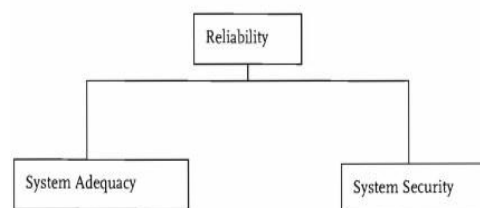


Figure 1: Reliability categories[3]

The Capacity to provide customers with existing generation and transmission infrastructure is the System's ability to supply load demand. Systems adequacy is assessed based on incident frequency, length, and probability [3]. System security refers to maintaining stable operating conditions despite changes like sudden unbalance in faults and equipment failures resulting in loss of system stability. System security is entirely dependent on system adequacy.

The assessment of the reliability of PV and composite power systems networks is fundamental to planning and operation [4]. It will also be essential to justify acceptable levels of penetration of PV, to evaluate the impact of PV resources on the efficiency and security of power systems, and to design energy storage to maximise the application of PV [2].

1.1. Aims of the Project

This project proposes an innovative framework for reliability improvement of essential infrastructures like transformer and transmission lines. The methodology is implemented using Markov modelling technique by adding photovoltaic sources and battery energy storage to critical load points. Reliability methods used in this work are analytical and simulative. Load point failure rates and annual average interruption duration is used for analysis.

1.2. Objectives

- To design PV Markov stochastic models using component repair and failure rates.
- To design BESS Markov stochastic models using the component repair and failure rates.
- To perform test case scenarios of critical load points with and without PV and BESS integration.
- To determine maximum penetration level of PV and BESS integration for reliability improvement.
- To use reliability indices SAIFI, SAIDI and ENS are used to evaluate reliability improvements.

1. Literature Review

Critical infrastructure reliability is vital for the secure operation of a power system and supplying the customers. Increased energy demand in conventional power systems results in power blackouts and unnecessary load shedding. Therefore, it is vital to monitor and devise methods to improve the reliability of critical power system components like transformers and heavily loaded lines[5]. Utilities have resorted to

integrate renewable energy sources to meet the demand and improve power system availability.

The task force on the reliability test system provides a detailed base model for composite system reliability studies[6],[7]. The report describes the load model, generating system, and transmission system. A reliability test model for educational purposes with all data is given in[8], which comprehensively analyses reliability indices for composite systems. In [9], energy storage and wind integration effects on generation-transmission power system reliability are evaluated with DC optimal power flow and monte Carlo simulation. Monte Carlo simulations are further used in [10],[11] in addition to artificial neural networks. Markov analytical modelling has been used in photovoltaic active distribution systems to determine failure and repair rates of photovoltaic and battery systems. Composite systems reliability considering solar irradiance and equipment availability is used in [12],[13]. The authors propose an analytical approach that captures the variability nature of solar power and equipment failures. Failure rate, outage duration, and expected energy not supplied of the grid-connected photovoltaic system are evaluated in [14]. State enumeration is used to perform reliability analysis of grid-connected photovoltaic considering intermittent power and critical components failure rates[15]. Markov modelling is used in determining repair and failure rates of the photovoltaic components and battery energy storage[2][16][6].

This paper proposes Markov modelling technique that captures solar intermittency and uncertainties of PV and BESS integration to composite systems reliability improvements. This is done by studying the improvement of critical points' reliability by integrating photovoltaic and strategic energy storage using reliability test system RTS-79. Hourly solar irradiance is used as input for power curve generation used in the model. Digsilent inbuilt photovoltaic system and battery energy storage are used. The states' probability and frequencies are determined using Markov chains for stochastic modelling in Digsilent.

The state enumeration technique is used for studies using the Digsilent reliability assessment tool. The calculated reliability indices, system average interruption frequency index (SAIFI), system average interruption duration index (SAIDI) and energy not supplied (ENS) is used to assess reliability improvements. This research gives maximum penetration levels capacity and strategic locations for reliability improvements of critical points.

2. The Technique and Component Modelling

1.1. Markov Modelling Technique

Markov modelling is useful for time series studies because of its flexibility. It is a stochastic process that uses a set of states to model the characteristics and behaviour. Markov modelling makes two major assumptions:[17]

- i) Memoryless system where the probability of states future is only dependent on the current state while neglecting the past conditions.
 - ii) Stationary system, which implies that states transition probabilities are constant and time-invariant.
- Reliability studies apply continuous Markov processes, which are continuously occurring with constant state transitions. Discrete methods consist of transition states with given time steps of occurrence.

1.1. Modelling Battery Energy Storage

The battery is essential in increasing the reliability of the power supply of photovoltaics. Battery energy storage contains a battery module and its controller. Markov model adopted is for a two-component repairable system, as shown in figure 3. The Markov model gives states transition process diagram, figure 3. Table 1 provides repair and failure rates used in Markov modelling processes.

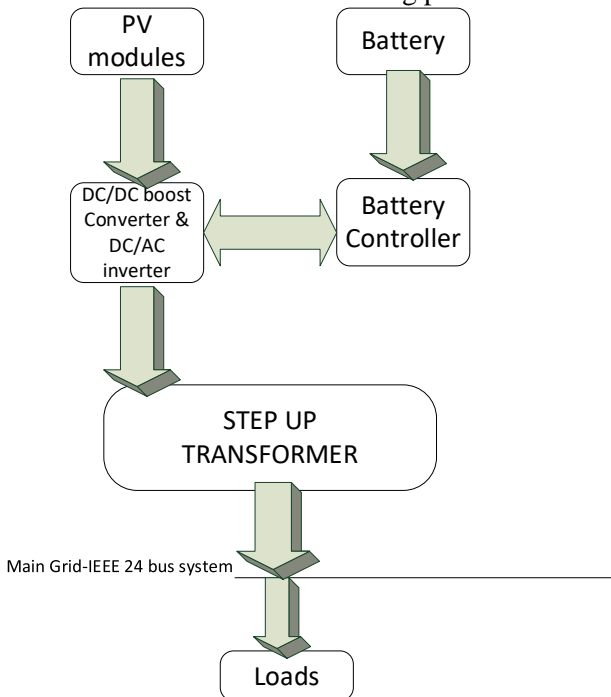


Figure 1: Main PV and Battery components

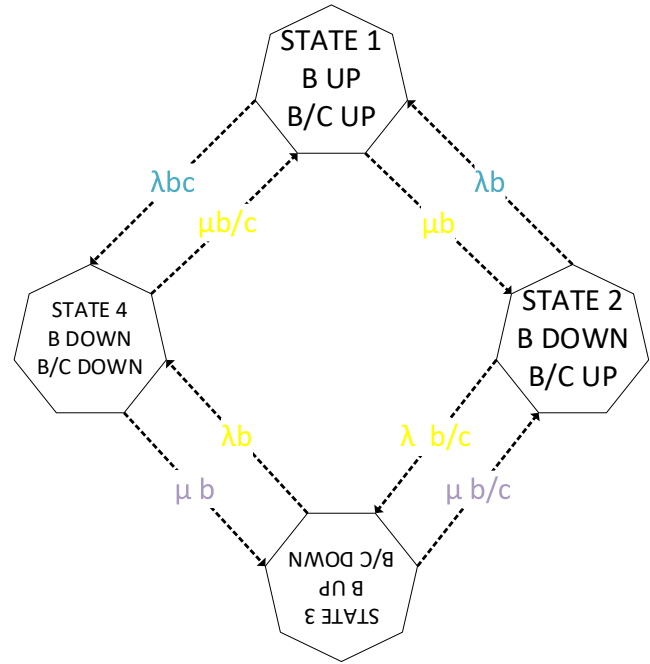


Figure 2: Stochastic Markov model of the two-component battery system

λ_B, μ_B is the failure and repair rates of the battery.

$\lambda_{B/C}, \mu_{B/C}$ is the failure and repair rates of the battery controller.

Table 1: Repair and failure rates for Battery Markov model[17]

Description	Failure rates (λ) (f/y)	Repair rates (μ) (r/y)
Battery	0.0312	51.9571
Battery charger	0.125	45.213

The transition matrix of the two-component repairable system is given by;

$$\begin{bmatrix}
 -(\lambda_1 + \lambda_2) & \mu_1 & \mu_2 & 0 \\
 \lambda_1 & -(\mu_1 + \lambda_2) & 0 & \mu_2 \\
 \lambda_2 & 0 & -(\mu_1 + \lambda_1) & \mu_1 \\
 0 & \lambda_2 & \lambda_1 & -(\mu_1 + \mu_2)
 \end{bmatrix}
 \begin{bmatrix}
 P_1 \\
 P_2 \\
 P_3 \\
 P_4
 \end{bmatrix}
 =
 \begin{bmatrix}
 0 \\
 0 \\
 0 \\
 0
 \end{bmatrix}$$

Since all the probabilities should add up to 1, the transition matrix is reduced as below.

$$\begin{bmatrix} 1 & 1 & 1 & 1 \\ \lambda_1 & -(\mu_1 + \lambda_2) & 0 & \mu_2 \\ \lambda_2 & 0 & -(\mu_1 + \lambda_1) & \mu_1 \\ 0 & \lambda_2 & \lambda_1 & -(\mu_1 + \mu_2) \end{bmatrix} \begin{bmatrix} P_1 \\ P_2 \\ P_3 \\ P_4 \end{bmatrix} = \begin{bmatrix} 1 \\ 0 \\ 0 \\ 0 \end{bmatrix} \quad (2)$$

The probabilities are solved using linear algebra, as shown.

$$P_1 = \frac{\mu_1 \mu_2}{(\mu_1 + \lambda_1)(\mu_2 + \lambda_2)}$$

$$P_2 = \frac{\lambda_1 \mu_2}{(\mu_1 + \lambda_1)(\mu_2 + \lambda_2)}$$

$$P_3 = \frac{\lambda_2 \mu_1}{(\mu_1 + \lambda_1)(\mu_2 + \lambda_2)}$$

$$P_4 = \frac{\lambda_1 \lambda_2}{(\mu_1 + \lambda_1)(\mu_2 + \lambda_2)}$$

This gives $P_1 = 99.6644$, $P_2 = 0.0595$, $P_3 = 0.2755$ & $P_4 = 0.000165$

$$f_1 = \frac{\mu_1 \mu_2 (\lambda_1 + \lambda_2)}{(\mu_1 + \lambda_1)(\mu_2 + \lambda_2)}$$

$$f_2 = \frac{\lambda_1 \mu_2 (\mu_1 + \lambda_2)}{(\mu_1 + \lambda_1)(\mu_2 + \lambda_2)}$$

$$f_3 = \frac{\lambda_2 \mu_1 (\lambda_1 + \mu_2)}{(\mu_1 + \lambda_1)(\mu_2 + \lambda_2)}$$

$$f_4 = \frac{\lambda_1 \lambda_2 (\mu_1 + \mu_2)}{(\mu_1 + \lambda_1)(\mu_2 + \lambda_2)}$$

The frequencies of the states are determined as $f_1 = 15.5676$, $f_2 = 3.1171$, $f_3 = 12.4648$, $f_4 = 0.0168$. The above probabilities and frequencies are inputs in stochastic modelling of the battery system in Digsilent.

1.2. Modelling Photovoltaic System

The photovoltaic system generates electricity by converting sunlight energy. Due to its renewable and economic nature, solar power is gaining popularity. Solar power output in photovoltaic is dependent on the solar intensity and temperature of the surroundings[13]. Due to variations in solar irradiance and temperature during various times, the photovoltaic output also varies.

The photovoltaic system consists of a boost converter, PV module, and inverter as represented in the schematics. Markov modelling is used to model the probabilities and frequencies of the states of each component.

Table 2 gives the failure and repair rates used in Markov modelling of components

Table 2: Failure and repair rates of PV Markov model[17]

Description	Failure rates (λ) (f/y)	Repair rates (μ) (r/y)
PV module	0.04	18.25
DC boost converter	0.152	55.232
DC/AC inverter	0.143	52.143

Since the PV module and DC boost converter are in series, repair and failure rates are summed as shown.

The inverter and converter assume the same Markov model as the battery. The failure and repair rates of the combined components are given as estimate below.

$$\lambda_{conv,inv} = [\lambda_{con} + \lambda_{inv}]$$

$$\lambda_{conv,inv} = 0.295 \left(\frac{f}{y}\right) \quad (3)$$

$$\mu_{conv,inv} = \frac{[\lambda_{conv} + \lambda_{inv}]}{\left[1 + \frac{\lambda_{conv}}{\mu_{conv}}\right] \left[1 + \frac{\lambda_{inv}}{\mu_{inv}}\right] - 1} \quad (4)$$

$$\mu_{conv,inv} = 53.617 \left(\frac{r}{y}\right)$$

Table 3: Reduced PV Markov Model

Description	Failure rates (λ) (f/y)	Repair rates (μ) (r/y)
PV	0.04	18.25
Converter-inverter	0.295	53.617

The probabilities and frequency of states are determined similarly to the battery model, and its Markov model is represented in figure 3.

λ_{PV}, μ_{PV} is the failure and repair rates of the photovoltaic module.

$\lambda_{Con/Inv}, \mu_{Con/Inv}$ is the failure and repair rates of the combined DC/DC boost converter and DC/AC inverter.

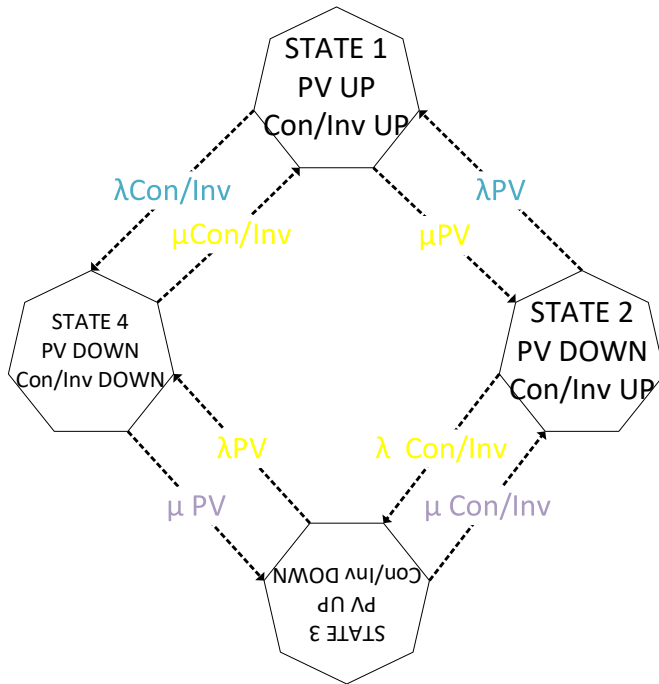


Figure 3: PV two-component Markov model

The states probabilities are given as:

$$P1 = 99.2353, P2 = 0.2175, P3 = 0.5456 \text{ \& } P4 = 0.00196$$

The frequencies of the states are determined as $f1 = 33.24, f2 = 4.06, f3 = 29.296, f4 = 0.086$.

Probability and frequency state values are used in Digsilent stochastic modelling of the Photovoltaic and battery systems.

3. Composite reliability system Assessment

Reliability analysis of composite systems is performed based on analytical methods, state enumeration, and Monte Carlo. Monte Carlo has the capability of modelling a wide range of operating conditions. This method involves the sampling of events randomly, and after that, analysis of each event sampled. Therefore, simulation of the system's actual and random behavior is used to estimate reliability indices. However, this method depends on the simulation of numerous events for realistic output and thus takes a longer time.

State Enumeration is highly advanced and has been used for a long time. This method evaluates reliability indices analytically by representing the system using mathematical models. It uses contingency enumeration to compute the accurate, reliable index. However, this method is not suitable for simulating large systems with different operating conditions.

The reliability of the composite system is measured by load point and system indices. The load points indicators provide reliability of specific individual bus lines that is essential to identify weaknesses and consequences for the

addition of local components. System indices provide summarized conditions of the entire power system under consideration.

Load point indices used include failure rate, average outage time, and average annual unavailability. Considering a load point at k^{th} .

$$\lambda_k = \frac{N_k}{\sum T_{upk}} \tag{5}$$

$$r_k = \frac{\sum T_{downk}}{N_k} \tag{6}$$

$$r_k = \frac{\sum T_{downk}}{N_k} \tag{7}$$

$$U_k = \frac{\sum T_{downk}}{\sum T_{downk} + \sum T_{upk}} \tag{8}$$

N_k represents the number of failures, $\sum T_{downk}$ is the total downtime, and $\sum T_{upk}$ is the total uptime at load point k . Load point indices are used to generate system indices as follows:

SAIFI

It gives the frequency at which a customer experiences interruption during the specific calculation period.

$$SAIFI = \frac{\sum \lambda_k C_k}{\sum C_k} \tag{9}$$

SAIDI

It gives the period of interruption duration to a customer during the calculation period.

$$SAIDI = \frac{\sum U_k C_k}{\sum C_k} \tag{10}$$

C_k is the k th load point number of customers.

ENS

It gives an average amount of energy not delivered to the system loads at any specific time under consideration.

$$EENS = \sum L_{ave k} * U_k \tag{11}$$

$L_{ave k}$ is the average customer, load interrupted by outage k .

4. Network Modelling and Reliability Assessment

IEEE reliability test system consisting of generation, transmission, and load model is adopted for test purposes. The system consists of 32 power plants with an output of between 12 and 400 MW and a total output of 3,405 MW.

The system includes 138 kV and 230 kV areas with 24 buses connected to 38 lines. For one year, the load model gives a maximum load per unit of 2 850 MW per annum. Data on the test system components are given in [7].

The solar power intermittency effects are modelled using Australian normalized photovoltaic output data. The PV and BESS are connected via a common bus before linking with a step-up transformer to the primary grid. Figure 5 shows the model connected to Bus 3 of the test system.

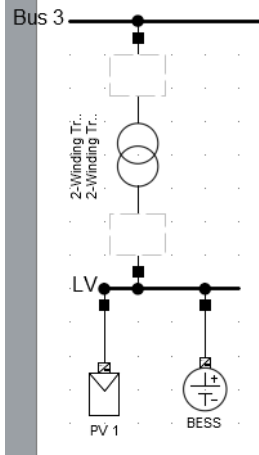


Figure 4: PV and BESS model Connection at Bus 3 in

Digsilent

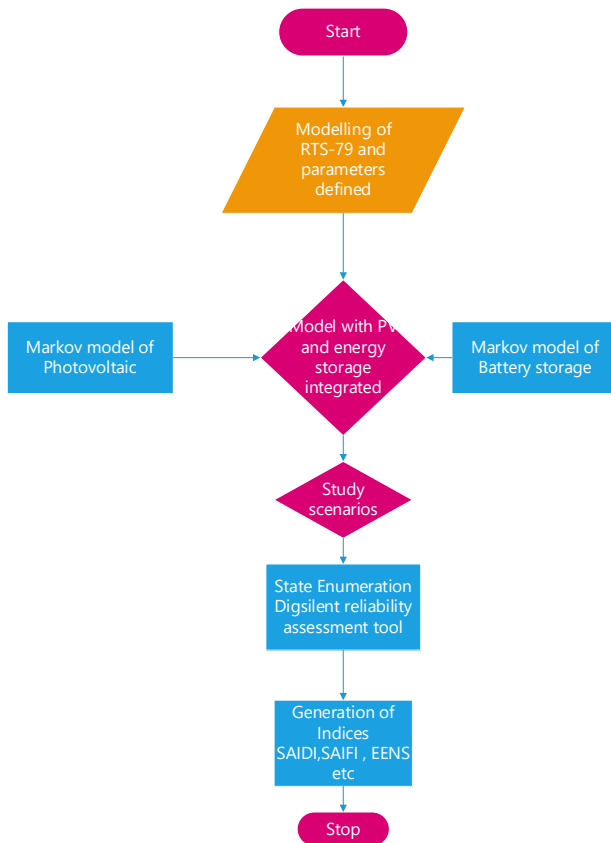


Figure 5: Model assessment flowchart.

6 Results and Discussion

6.1 Load Point Indices

This case study analyses load points indices of PV and BESS integration. The reliability indices of interest are interruption frequency, interruption time, interruption duration, and load point energy not supplied. The chosen buses are selected by considering energy not supplied index and voltage profile from load flow studies. Load point indices reduce after replacing conventional generation with PV and energy storage, as shown in appendix, table 6. Bus 2,15 and 16 register improvement of 37%,64%, and 43% of load point energy not supplied. The reduction in load point indices can be attributed to solar resources and energy storage availability in the network. The interruption frequency and time for buses 14 and 16 remained constant. Bus 14 is connected with synchronous compensator which balances the power deficits as it arises. The load point indices are then used in computing the bus indices, as shown in table 2.

Table 4: Critical points SAIFI, SAIDI and ENS indices.

Bus	SAIDI (h/Ca)		SAIFI (1/Ca)		ENS (MWh/a)		
	Base	New	Base	New	Base	New	% d
1	0.1498	0.1251	2.847	2.377	32.560	27.192	16.49
2	0.1498	0.1251	2.847	2.377	29.244	24.422	16.49
15	0.1530	0.1277	1.989	1.660	66.778	55.738	16.53
7	0.0757	0.051	1.438	0.969	19.042	12.828	32.63
13	0.1277	0.1024	1.660	1.331	46.595	37.366	17.66
14	0.1024	0.0771	1.331	1.002	27.355	20.599	24.70
16	0.1530	0.1277	1.989	1.660	21.065	17.583	16.53

The bus system reliability indices decrease as conventional generation is replaced with PV and energy storage, as shown in table 4. Bus 7 had the highest improvement index of 32.63%, and bus 1&2 had the least with 16.49%. Thus, after the addition of PV and BESS, the reliability indices improve. For example, ENS of the listed buses gives an improvement of beyond 16.49%. It thus highlights the benefit of distributed generation of PV and decentralized energy storage to the network. However, the abnormal profile of solar energy during different times of the day comes with power uncertainty. It's expected during months with fewer sunshine hours, there will be an inadequate power supply, and standby power is needed to avoid

complete network failure.

6.2 PV and BESS penetration levels

The IEEE 24 bus system is modelled as in [7], and the base case results are obtained. The penetration percentage level is achieved by substituting conventional generation with PV and BESS as part of the system's total load. The integration point is identified as being critical based on load point energy not supplied and voltage profile levels.

The transmission reliability expected energy not supplied (ENS) for base model RTS-79 is 1053.14 MWh/year[18]. However, this study's modelled 24 bus system gives an ENS value of 994.767 MWh/year, which is a deviation of -5.5%. Digsilent is a modern software with improved accuracy with different capabilities. The simulation neglected protection switching failures and double earth faults in the studies.

Table 5: PV and BESS penetration levels system reliability indices.

Penetration level (%)	SAIFI (1/Ca)	SAIDI (h/Ca)	ENS (MWh/a)
0	4.113824	59.485	994.767
2.8	4.064412	58.546	984.5752
4.9	4.039118	58.217	973.5355
7.6	4.014412	57.748	967.3240
13	3.989118	57.419	963.8408
18.5	3.963824	57.090	952.8005
25.5	3.938529	56.761	943.5704
32.5	3.938529	56.761	943.5704

From the table 5, the maximum penetration of PV and BESS is 25.5 %. For these penetration levels, the SAIFI improves by 4.26%, SAIDI by 4.58%, and ENS by 5.1% compared with the base case. Therefore, for this network, the recommended PV and BESS penetration level is 25.5%. However, if greenhouse gas emissions reductions are the priority, the penetration level can be increased to 32.5% since reliability indices remain constant. Further increase in penetration levels above 32.5% leads to network saturation, and the system fails.

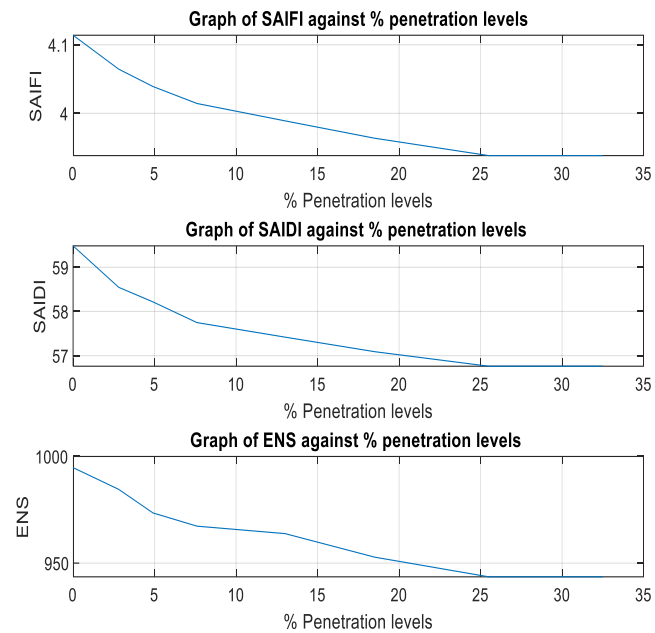


Figure 6: SAIFI, SAIDI & ENS against Penetration levels

From the graphs presented, the SAIFI, SAIDI, and ENS indices follow a downward decreasing trend. It indicates an improvement in reliability indices as the PV and BESS penetration levels is increased gradually. However, it is evident the maximum penetration level sustained by the system before failure is 32.5%. This phenomenon can be attributed to the intermittency of the solar power availability integrated into the system. The chances of the loads demand exceeding generation levels increases at some points due to constant zero generations.

6.1 PV and BESS different sections integrations

This case involved the integration of PV and BESS into buses 21,18,9,10,7 and 2. These were identified as critical buses focusing on the load point energy not supplied index and voltage profile levels. Bus 18, which serves as a system slack bus, a reference bus registered a negative improvement of its indices. However, the rest buses recorded a positive improvement as shown in the table 7 and fig.8. The SAIFI and SAIDI indices at all buses remain constant. Thus, integrating PV and BESS to any point in the system does not affect SAIFI and SAIDI. Bus 21 gives the most remarkable ENS improvement of 1.02 %, and Bus 10 the least with 0.05%. The reason is that the bus ten network is congested, with line 10 exceeding the line capacity. Increased penetration of PV and BESS from the

bottom section of the network results in transmission lines congestions as compared with upper sections of bus 21. As a result, line capacity is exceeded leading to decreasing ENS reliability index at the specific integration location.

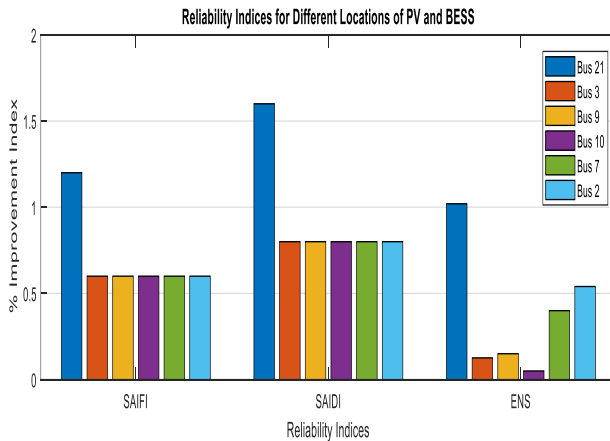


Figure 7: Different locations of PV and BESS integrations

It is thus evident that the location of PV and BESS influence the reliability of the system. The main reason is that different PV and BESS locations result in the system's additional power flow depending on load and generation points. This difference in power flows results in the difference in the reliability indices accordingly. Therefore, the reliability improvement of critical infrastructure, the site of the location of PV and BESS needs to be taken into consideration in a composite system.

6 Conclusion

This work has presented Markov modelling technique for photovoltaic and battery energy storage to improve reliability of critical infrastructures. The framework designed captures intermittency and uncertainties related to solar power generation.

In many case studies, the Markov model is employed to capture genuine properties of PV generation and BESS. The study results give a clear indication that strategic connection of PV and BESS results to reliability improvement of critical points and the entire system. However, high penetration levels result to reduced reliability due to network stressing and congestion. For this system, maximum allowable penetration levels are 32.5% above, which system fails due to excessive congestion and abnormal profile of solar power output.

Case studies suggest that interruptions duration and frequency are similar for PV and BESS different locations. However, the ENS value differs from one location to another quantifying the benefits of strategic integration to reliability improvements of critical points.

The proposed Markov model can be used for benchmark studies for PV penetration levels reliability, adequacy assessments and impacts.

7 Future Works

The method used in reliability analysis in this paper is state enumeration-based reliability assessment in Digsilent reliability assessment tool. However, studies can be extended to using of Monte Carlo simulation method to compare the results obtained and any deviations.

Simulation of the ageing effects on the composite system reliability with the integration of PV and BESS. It will be a base point in estimating project lifetime and viability for investment in the long run.

8 Acknowledgments

The work above was possible through Chevening Scholarship which is a program focused on mentoring future leaders across the world. Therefore, I am forever grateful for Chevening and University of Birmingham for the wonderful opportunity and experience.

I would like to thank Dr. Dilan Jayaweera, Senior lecturer, Department of electrical and electronics for his continued support as my leading supervisor during the entire project period.

9 References

- [1] K. M. Zuev and M. Beer, "Reliability of Critical Infrastructure Networks: Challenges," no. January, pp. 71–82, 2018, doi: 10.1061/9780784415139.ch06.
- [2] P. Zhang, W. Li, S. Li, Y. Wang, and W. Xiao, "Reliability assessment of photovoltaic power systems: Review of current status and future perspectives," *Appl. Energy*, vol. 104, pp. 822–833, 2013, doi: 10.1016/j.apenergy.2012.12.010.
- [3] S. Bhattacharyya, "The influence of a 'Hybrid Grid' on the network's power quality and reliability," Eindhoven University of Technology, 2006.
- [4] H. Kim and C. Singh, "Composite power system reliability modeling and evaluation considering aging components," *ELECO 2009 - 6th Int. Conf. Electr. Electron. Eng.*, pp. 14–18, 2009.
- [5] J. Johansson, H. Hassel, and E. Zio, "Reliability and vulnerability analyses of critical infrastructures: Comparing two approaches in the context of power systems," *Reliab. Eng. Syst. Saf.*, vol. 120, pp. 27–38, 2013, doi: 10.1016/j.ress.2013.02.027.
- [6] C. Grigg and P. Wong, "The IEEE reliability test system -1996 a report prepared by the reliability test system task force of the application of probability methods subcommittee," *IEEE Trans. Power Syst.*, vol. 14, no. 3, pp. 1010–1020, 1999, doi: 10.1109/59.780914.
- [7] P. M. Subcommittee, "IEEE Reliability Test System," in *IEEE Transactions on Power Apparatus and Systems*, vol. PAS-98, no. 6, pp. 2047–2054, Nov. 1979, doi: 10.1109/TPAS.1979.319398..
- [8] R. Billinton *et al.*, "A reliability test system," *Power*, vol. 4, no. 3, pp. 1238–1244, 1989.
- [9] P. Gautam and R. Karki, "Quantifying Reliability Contribution of an Energy Storage System to a Distribution System," *IEEE Power Energy Soc. Gen. Meet.*, vol. 2018-Augus, pp. 2–6, 2018, doi: 10.1109/PESGM.2018.8586222.
- [10] J. Choi, S. Moon, H. Kim, B. Lee, and R. Billinton, "Development of the ELDC and reliability evaluation of composite power system using Monte Carlo method," *Proc. IEEE Power Eng. Soc. Transm. Distrib. Conf.*, vol. 4, no. c, pp. 2063–2068, 2000, doi: 10.1109/pess.2000.866964.
- [11] R. Billinton, "System Reliability Analysis With Time Varying Loads," *Power*, vol. 10, no. 3, pp. 1540–1545, 1995.
- [12] S. Sulaeman, M. Benidris, and J. Mitra, "Modeling and assessment of PV solar plants for composite system reliability considering radiation variability and component availability," *19th Power Syst. Comput. Conf. PSCC 2016*, 2016, doi: 10.1109/PSCC.2016.7540983.
- [13] T. Tuffaha and M. Almuhaeni, "Reliability assessment of a microgrid distribution system with pv and storage," *Proc. - 2015 Int. Symp. Smart Electr. Distrib. Syst. Technol. EDST 2015*, pp. 195–199, 2015, doi: 10.1109/SEDST.2015.7315206.
- [14] Y. Guo-hua, "Power Based on Monte Carlo Method," *Power Eng. Autom. Conf. (PEAM), 2011 IEEE*, vol. 1, pp. 92–95, 2011.
- [15] P. Zhang, Y. Wang, W. Xiao, and W. Li, "Reliability evaluation of grid-connected photovoltaic power systems," *IEEE Trans. Sustain. Energy*, vol. 3, no. 3, pp. 379–389, 2012, doi: 10.1109/TSTE.2012.2186644.
- [16] S. Su, Y. Hu, L. He, K. Yamashita, and S. Wang, "An Assessment Procedure of Distribution Network Reliability Considering Photovoltaic Power Integration," *IEEE Access*, vol. 7, pp. 60171–60185, 2019, doi: 10.1109/ACCESS.2019.2911628.
- [17] A. T. Mohamed, A. A. Helal, and S. M. El Safty, "Distribution System Reliability Evaluation in Presence of DG," *Proc. - 2019 IEEE Int. Conf. Environ. Electr. Eng. 2019 IEEE Ind. Commer. Power Syst. Eur. IEEEIC/I CPS Eur. 2019*, 2019, doi: 10.1109/IEEEIC.2019.8783657.
- [18] J. M. S. Pinheiro, "Probing the new ieee reliability test system (rts-96): hl-ii assessment," *IEEE Trans. Power Syst.*, vol. 13, no. 1, pp. 171–176, 1998, doi: 10.1109/59.651632.

10 Appendices

Table 6: Load Point Indices of critical points.

Bus	AIT (h/a)			AIF (1/a)			AID (h)			LPENS (MWh/a)		
	Base	New	%d	Base	New	%d	Base	New	%d	Base	New	%d
1	71.03	63.05	11	4.29	3.87	9.8	16.56	16.30	1.6	47.8	42.41	11
2	71.03	63.05	11	4.29	3.87	9.8	16.56	16.30	1.6	42.9	26.67	37
15	56.45	50.86	9.9	4.34	3.91	9.9	13.0	13.0	0	111.5	40.17	64
7	156.8	148.8	5.1	12.46	12.0	3.4	12.58	12.36	1.8	122.1	115.9	5
13	50.86	45.27	11	3.91	3.48	11	13.0	13.0	0	83.96	74.73	11
14	45.27	45.27	0	3.48	3.48	0	13.0	13.0	0	54.71	54.71	0
16	56.45	56.45	0	4.34	4.34	0	15.97	13.0	19	61.75	35.17	43

d-difference

Table 4: Integration of PV and BESS in different locations

Index	Base case	Bus 21	Bus 18	Bus 3	Bus 9	Bus 10	Bus 7	Bus 2
SAIFI (1/Ca)	4.1138	4.0644	4.4944	4.0891	4.0891	4.0891	4.0891	4.0891
SAIDI (h/Ca)	59.4848	58.546	64.136	59.0154	59.0154	59.0154	59.0154	59.0154
ENS (MWh/a)	994.767	984.576	1083.83	993.514	993.276	994.2561	990.791	989.384

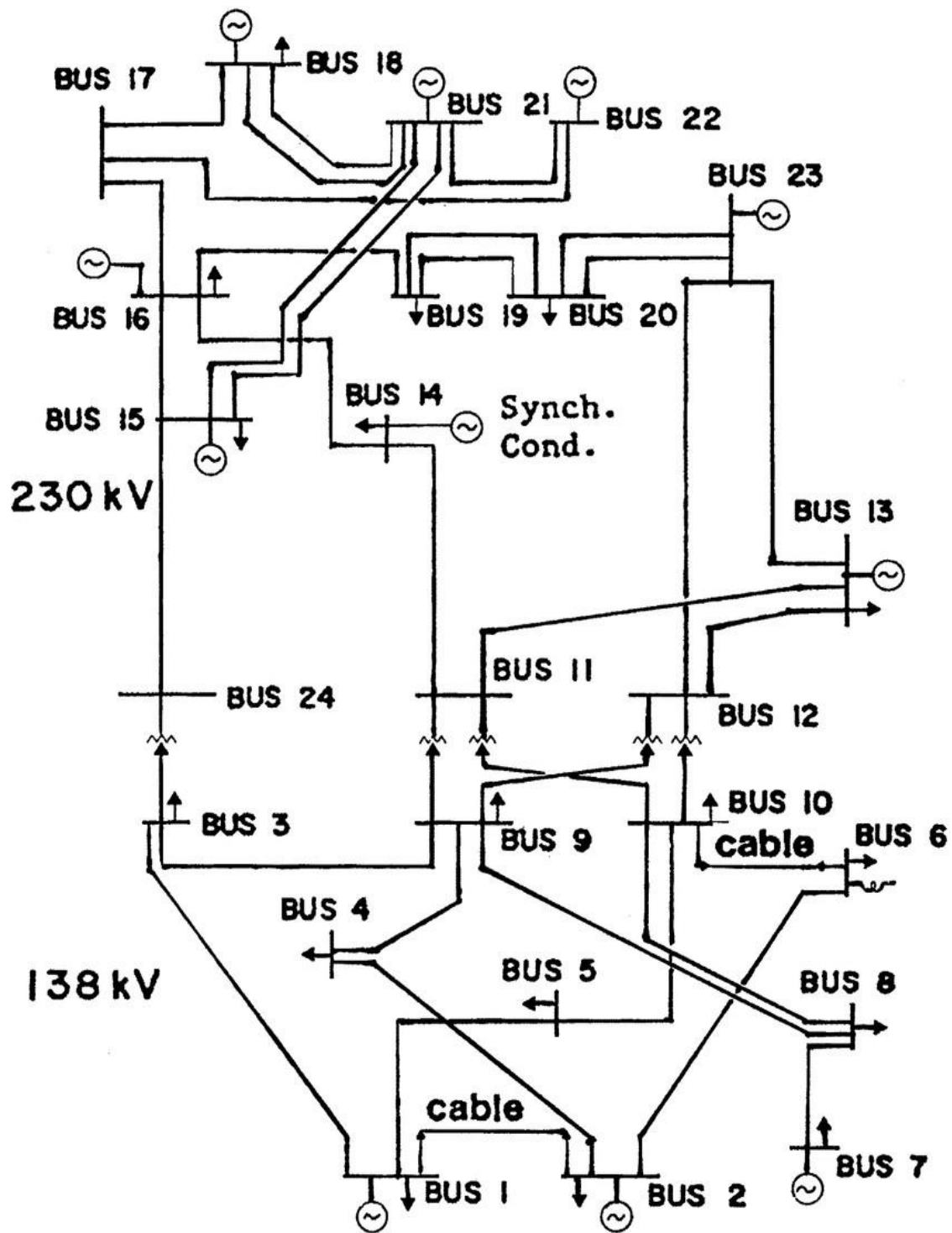


Figure 9: IEEE 24 bus system configuration [7]

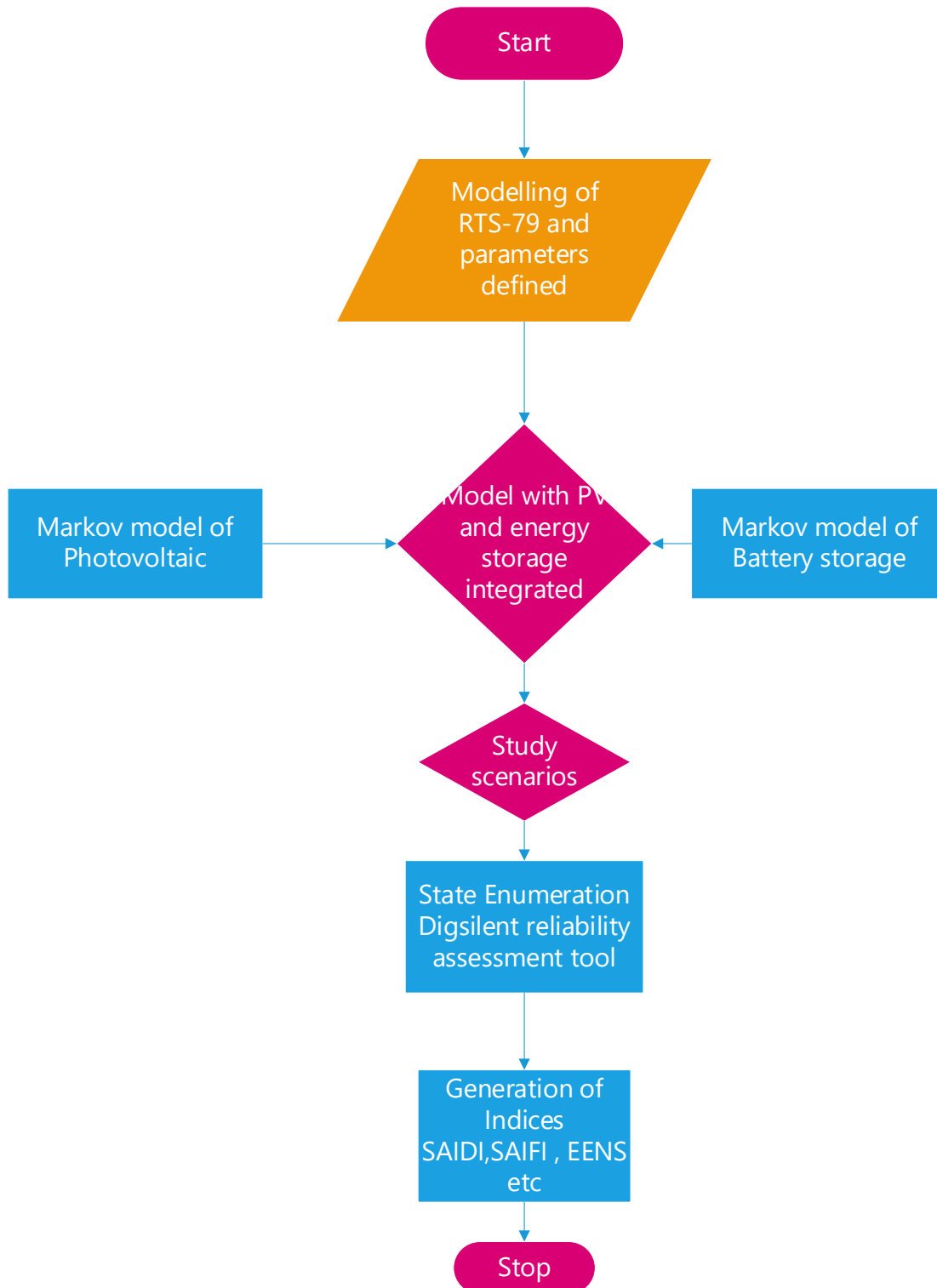


Figure 10: Model assessment flowchart.

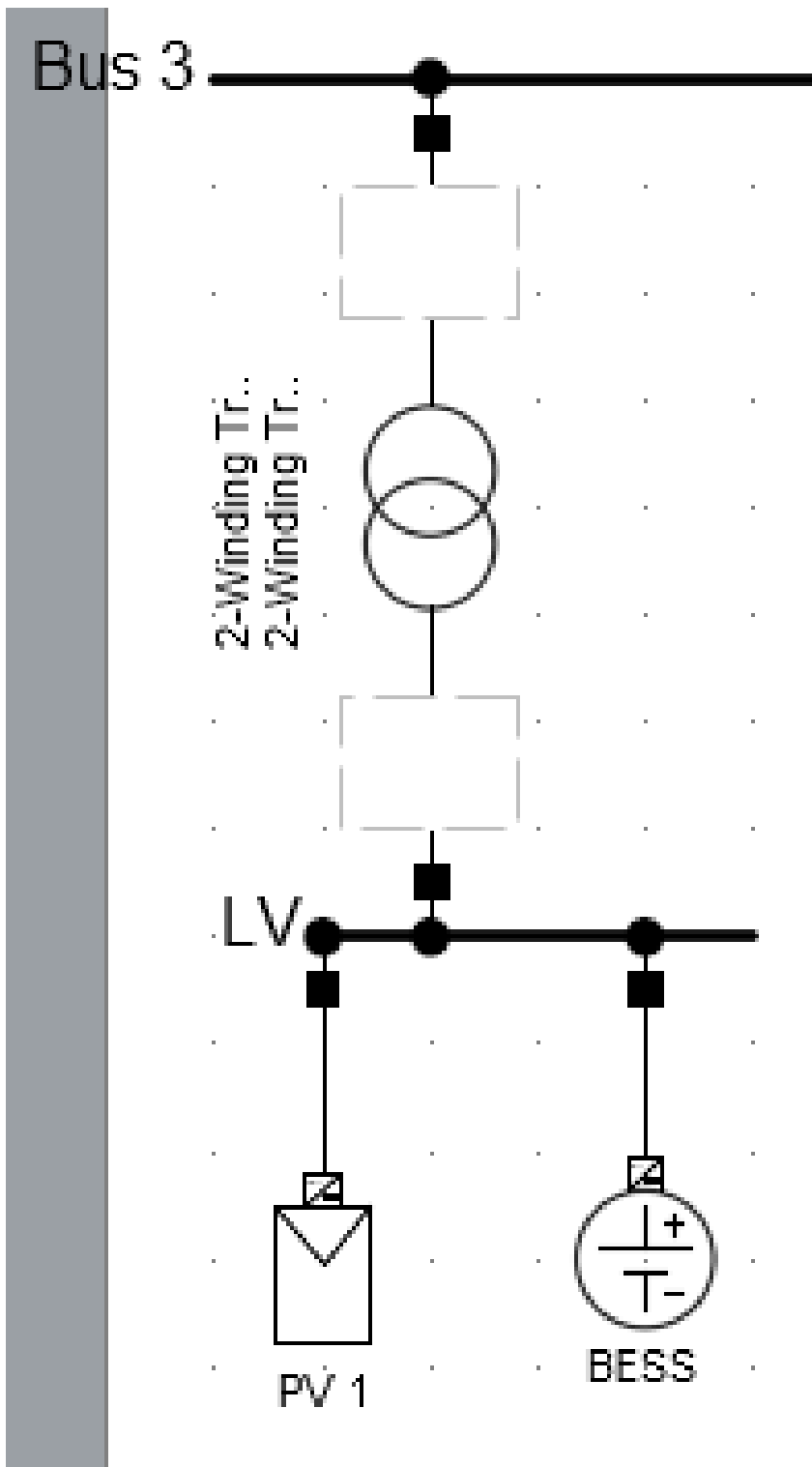


Figure 11: PV and BESS model Connection at Bus 3 in Digsilent.

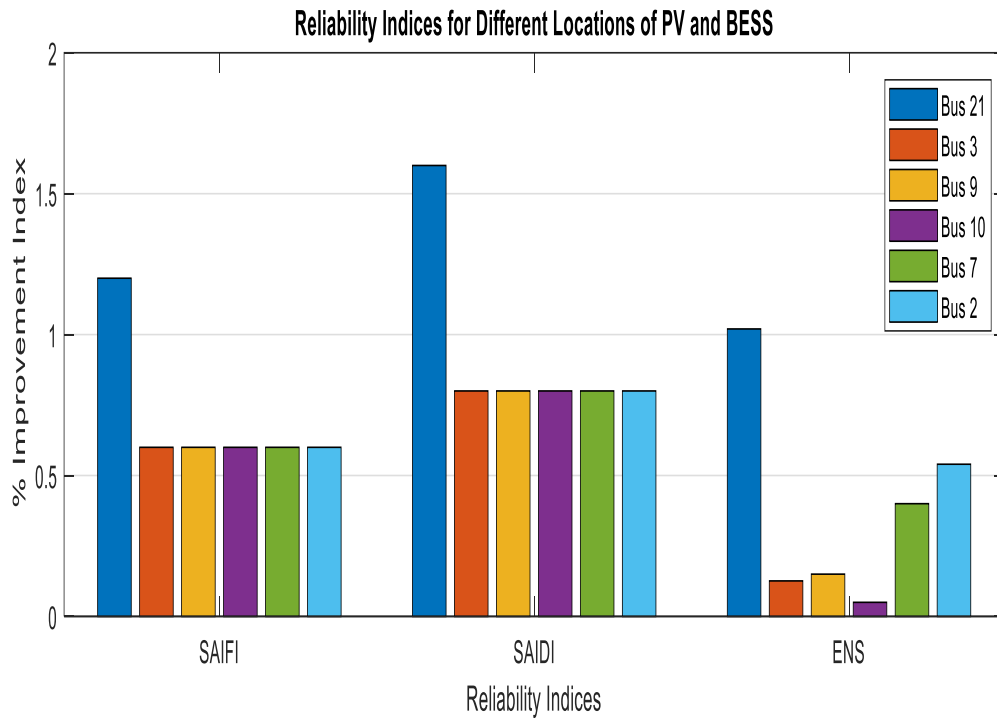


Figure 12: Different locations of PV and BESS integrations

Table 6: Load Point Indices of critical points.

Bus	AIT (h/a)			AIF (1/a)			AID (h)			LPENS (MWh/a)		
	Base	New	%d	Base	New	%d	Base	New	%d	Base	New	%d
1	71.03	63.05	11	4.29	3.87	9.8	16.56	16.30	1.6	47.8	42.41	11
2	71.03	63.05	11	4.29	3.87	9.8	16.56	16.30	1.6	42.9	26.67	37
15	56.45	50.86	9.9	4.34	3.91	9.9	13.0	13.0	0	111.5	40.17	64
7	156.8	148.8	5.1	12.46	12.0	3.4	12.58	12.36	1.8	122.1	115.9	5
13	50.86	45.27	11	3.91	3.48	11	13.0	13.0	0	83.96	74.73	11
14	45.27	45.27	0	3.48	3.48	0	13.0	13.0	0	54.71	54.71	0
16	56.45	56.45	0	4.34	4.34	0	15.97	13.0	19	61.75	35.17	43

d-difference

Table 4: Integration of PV and BESS in different locations

Index	Base case	Bus 21	Bus 18	Bus 3	Bus 9	Bus 10	Bus 7	Bus 2
SAIFI (1/Ca)	4.1138	4.0644	4.4944	4.0891	4.0891	4.0891	4.0891	4.0891
SAIDI (h/Ca)	59.4848	58.546	64.136	59.0154	59.0154	59.0154	59.0154	59.0154
ENS (MWh/a)	994.767	984.576	1083.83	993.514	993.276	994.2561	990.791	989.384